Interaction of Carbon Monoxide with the Apoptosis-Inducing Cytochrome c-Cardiolipin Complex

6 AUTHORS, INCLUDING:

Ivan Husu
Formerly Italian Natl. Res. Council (CNR, 20…
21 PUBLICATIONS   **163** CITATIONS

SEE PROFILE

Ursula Liebl
MINES ParisTech
84 PUBLICATIONS   **1,809** CITATIONS

SEE PROFILE

Michael Thomas Wilson
University of Essex
302 PUBLICATIONS   **7,953** CITATIONS

SEE PROFILE

Marten H Vos
École Polytechnique
142 PUBLICATIONS   **3,665** CITATIONS

SEE PROFILE

BIOCHEMISTRY
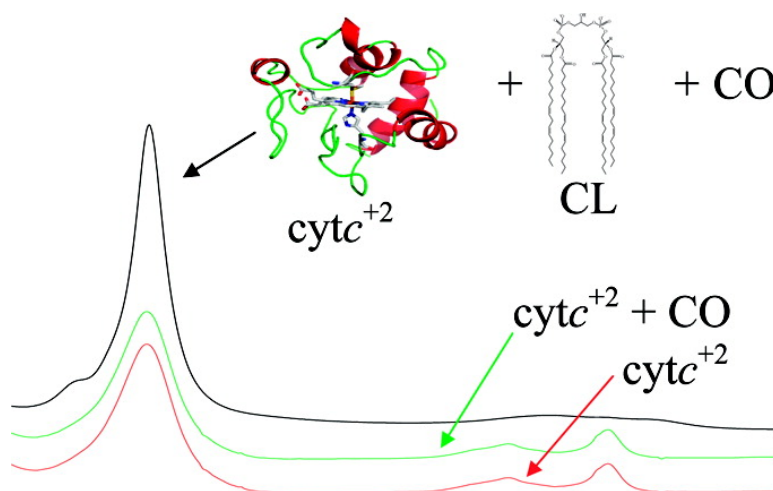## including biophysical chemistry & molecular biology

Article

Interaction of Carbon Monoxide with the Apoptosis-Inducing Cytochrome *c*#Cardiolipin Complex

Sofia M. Kapetanaki, Gary Silkstone, Ivan Husu, Ursula Liebl, Michael T. Wilson, and Marten H. Vos

More About This Article

Additional resources and features associated with this article are available within the HTML version:

- Supporting Information
- Access to high resolution figures
- Links to articles and content related to this article
- Copyright permission to reproduce figures and/or text from this article

View the Full Text HTML

ACS Publications
High quality. High impact.

Interaction of Carbon Monoxide with the Apoptosis-Inducing Cytochrome *c*−Cardiolipin Complex[†]

Sofia M. Kapetanaki,[‡,§,ll] Gary Silkstone,[‡,⊥] Ivan Husu,[⊥] Ursula Liebl,[§,ll] Michael T. Wilson,[⊥] and Marten H. Vos*[,§,ll]

Laboratoire d'Optique et Biosciences, CNRS, Ecole Polytechnique, and INSERM U696, F-91128 Palaiseau, France, and Department of Biological Sciences, University of Essex, Wivenhoe Park, Colchester CO4 3SQ, United Kingdom

Received September 24, 2008; Revised Manuscript Received January 13, 2009

ABSTRACT: The interaction of mitochondrial cytochrome (cyt) *c* with cardiolipin (CL) is involved in the initial stages of apoptosis. This interaction can lead to destabilization of the heme−Met80 bond and peroxidase activity [Basova, L. V., et al. (2007) *Biochemistry 46*, 3423−3434]. We show that under these conditions carbon monoxide (CO) binds to cyt *c*, with very high affinity ($\sim5 \times 10^7$ M^{-1}), in contrast to the native cyt *c* protein involved in respiratory electron shuttling that does not bind CO. Binding of CO to the cyt *c*−CL complex inhibits its peroxidase activity. Photodissociated CO from the cyt *c*−CL complex shows <20% picosecond geminate rebinding and predominantly bimolecular rebinding, with a second-order rate constant of $\sim10^7$ M^{-1} s^{-1}, an order of magnitude higher than in myoglobin. These findings contrast with those of Met80X mutant cyt *c*, where picosecond geminate recombination dominates due to the rigidity of the protein. Our data imply that CL leads to substantial changes in protein conformation and flexibility, allowing access of ligands to the heme. Together with the findings that (a) ~30 CL per cyt *c* are required for full CO binding and (b) salt-induced dissociation indicates that the two negative headgroup charges interact with ~5 positive surface charges of the protein, these results are consistent with a CL anchorage model with an acyl chain impaled in the protein [Kalanxhi, E., and Wallace, C. J. A. (2007) *Biochem. J. 407*, 179−187]. The affinity of CO for the complex is high enough to envisage an antiapoptotic effect of nanomolar CO concentrations via inhibition of the cyt *c* peroxidase activity.

Eukaryotic cytochrome (cyt)[1] *c* is a small water-soluble globular heme-containing protein that is located within the compartment between the inner and outer mitochondrial membranes. This protein has recently become the focus of considerable interest because of its role in linking two essential but very different cellular processes. As a redox component of the mitochondrial electron transfer chain it ferries electrons between the bc_1 complex and the terminal acceptor, cytochrome *c* oxidase. Here, the heme is axially coordinated by His and Met, and the protein is relatively rigid (*1, 2*), in agreement with its electron transfer function. In addition to this well-known function it is also now recognized to be central to at least two apoptotic processes. Thus cyt *c* holds a pivotal position linking the redox chemistry driving oxidative phosphorylation that produces ATP with a multifaceted major process in cellular physiology leading to programmed cell death, itself energy requiring.

Release of cyt *c* from the mitochondria into the cytoplasm triggers apoptosis through a mechanism that involves interaction with Apaf-1, pro-caspase-9, and dATP/ATP (*3*). A second process, recently proposed by Kagan and co-workers, is based on the interaction of cyt *c* with cardiolipin (CL) *prior to* its release from the mitochondrion (*4−6*). CL is found almost exclusively in the inner mitochondrial membrane, where this anionic phospholipid accounts for $\sim15−25\%$ of all phospholipids (*7, 8*). It is mainly located in the inner surface of the inner mitochondrial membrane with, however, a substantial portion of the total confined to the cytoplasmic side of the membrane (*8*). Upon interaction with CL, cyt *c* has been shown to change its tertiary structure, disrupt the heme−Met bond, drastically reduce its midpoint potential out of the range required for its role in the respiratory chain, and display a peroxidase activity instead. The latter leads to the oxidation of CL and subsequently to permeabilization of the outer mitochondrial membrane (*4, 5*).

The signaling molecules NO and CO are known to influence apoptosis (*9, 10*). NO can inhibit the peroxidase activity of the cyt *c*−CL complexes, and its access to the heme site is presumably facilitated by the presence of CL (*6*). During apoptosis, cyt *c* is released into the cytoplasm, at least partly in a nitrosylated form (*11*).

CO has versatile properties as both a signaling mediator and a regulator of important physiological processes (*12*). It is endogenously produced during the oxidative catabolism of heme by heme oxygenase (HO). The recent discovery of

[1] Abbreviations: CL, cardiolipin; cm, carboxymethyl; cmc, critical micelle concentration; cyt, cytochrome; EtOH, ethanol; HO, heme oxygenase; PC, phosphatidylcholine.

HO in liver mitochondria (*13*), regulating the mitochondrial heme pool, the protein heme content, and the production of reactive oxygen species is consistent with the participation of CO in cell signaling and life and death programs (*12*).

In contrast to NO, CO cannot bind to cyt *c* under physiological pH conditions (*14*). Chemical or genetic modification of cyt *c* that removes Met ligation makes the heme accessible for CO binding. However, in these modified proteins the CO remains largely kinetically sequestered in the heme environment (*15, 16*), and exchange between the heme pocket and the protein environment is poor, especially in comparison with typical ligand-binding heme proteins such as myoglobin. The dynamics of the heme−CO interaction were also found to be a sensitive probe of the heme environment, in much the same way as the dynamics of heme−NO interaction are for myoglobin (*16*).

The interactions of CO with the cyt *c*−CL complex have not previously been studied. In this work, we provide evidence for surprisingly facile binding of the physiological ligand CO to the ferrous cyt *c*−CL complex. We have characterized the binding properties of the complex by time-resolved absorption spectroscopy on the femtosecond to millisecond time scale. Our results support a model in which the binding of CL to ferric cyt *c* followed by reduction of the heme iron provides direct access for external gaseous ligands to bind. We argue that the cyt *c*−CO interaction may play a regulatory role in the early stages of apoptosis.

MATERIALS AND METHODS

Cyt *c* (horse heart) was purchased from Aldrich. Unless indicated otherwise, all experiments were carried out at pH 7.4 in Hepes buffer, 20 mM. Ferric cyt *c* was prepared by addition of potassium ferricyanide (1 mM) to cyt *c* (∼0.1 mM) followed by passage down a Sephadex G-25 column (size exclusion chromatography) to separate the mixture. Ferri-cyt *c* concentrations were calculated using the extinction coefficient of 106000 M^{-1} cm^{-1} at 410 nm (*17*). Protein concentrations were typically between 1 and 13 mM. CL (sodium salt from bovine heart) was purchased from Aldrich, and stock solutions were commonly ∼5 mM dissolved in EtOH and were freshly prepared or stored at −20 °C under N$_2$ to avoid oxidation. Aliquots of the CL stock solution were added to the (ferric) cyt *c* solution. The final concentration of EtOH in a protein sample was kept to a minimum (commonly ∼2%, not exceeding 5%) to avoid denaturation of the protein (see Results). Oleate (sodium salt) was purchased from Aldrich, and stock concentrations were commonly 20 mM dissolved in H$_2$O. The cyt *c*−CL complex was reduced either by addition of a few grains of sodium dithionite to degassed protein solution in the presence of ∼10^{-9} M catalase (to prevent the heme being bleached by peroxide generated through the reaction of dithionite with any remaining oxygen (*18*)) or by adding a degassed dithionite solution to a final concentration of 1 mM. The CO-bound form was subsequently formed by equilibration of the ferrous cyt *c*−CL complex with 1 atm of CO.

For preparation of phosphatidylcholine (PC)/CL liposomes, PC and CL were dissolved in 99.9% chloroform and 99.9% methanol (2:1 v/v), and the solvent was removed using rotary evaporation at room temperature (∼22 °C). To the lipid film was added degassed buffer; the total phospholipid concentra-

tion was 3.5 mM (2.5 and 1 mM in PC and CL, respectively). Argon gas was added to the mixture in the vessel, resulting in a slight positive pressure. Multilamellar phospholipid vesicles were produced by sonication of the containing vessel in a sonication bath for about 5 min. Ebselen (2-phenyl-1,2-benzisoselenazol-3(2*H*)-one, Sigma, final concentration 25 μM) was added to the liposomes prior to incubation with cyt *c* to prevent oxidative modification of the lipids. Ferri-cyt *c* (5 μM) was incubated with varying amounts of PC/CL liposomes (5:2) for about 2 h, and a minimum of dithionite and an excess of pure CO were then added to each sample, and spectra of the ferri, ferro, and CO forms were recorded. (Catalase was added to each sample prior to the addition of dithionite to remove any peroxide generated.)

Static absorption spectra were taken with a Cary 5E (Varian) spectrometer. Stopped-flow spectroscopy was carried out on an Applied Photophysics SX-20 instrument. Microsecond laser flash photolysis measurements were carried out on an Applied Photophysics (LKS.60) instrument. Carbon monoxide solutions of known concentrations were prepared by dilution of a stock, CO (1 atm) saturated buffer, the CO concentration of which was determined by titration against known concentrations of deoxymyoglobin (horse heart; Sigma). Second-order rate constants were determined from the slopes of plots of observed pseudo-first-order rate constants versus [CO]. The protein concentrations were typically between 2.5 and 5 μM and the experiments conducted under pseudo-first-order condition.

Multicolor femtosecond absorption spectroscopy using 60 fs pulses centered at 560 nm and white light continuum probe pulses in the 380−480 nm region, at a repetition rate of 30 Hz, and data analysis were performed as described (*16*).

Dynamic light scattering measurements on a filtered (450 nm) CL buffer solution (4.5% EtOH) were carried out using a Zetasizer Nano ZS (Malvern Instruments).

All ultrafast experiments were carried out at 21 °C and, unless indicated otherwise, all other experiments at 25 °C.

RESULTS

Addition of CL to ferri-cyt *c* bleaches the 695 nm absorption band (Figure 1A), indicating that interaction between the ferric protein and the phospholipid leads to rupture of the Fe−Met bond, in agreement with a former study (*5*). On addition of sodium dithionite to the ferri-cyt *c*−CL complex the ferro-cyt *c*−CL derivative is formed. This species is characterized by an absorption spectrum (Figure 1A) distinctly different from that of the ferrous protein in the absence of CL but reminiscent of the high-spin ferrous forms of Met80X mutants of cyt *c* and of carboxymethyl (cm) cyt *c* in respect to its flatter and broader line shape (*19, 20*). Also, the spectrum of the ferrous cyt *c*−CL complex, in both the Soret and visible regions, is essentially identical to spectra reported for microperoxidases, cyt *c*−SDS complexes, and cyt *c′*, which have been assigned as high-spin pentacoordinated *c*-type heme with His as the fifth ligand (*21−23*).

As shown in the inset to Figure 2, at pH ∼7, the ferrous native protein does not bind CO to any appreciable extent (it only does so at pH 13 or above and then relatively slowly (*14*)). We found this behavior to be in stark contrast to that of the cyt *c*−CL complex (Figure 1A), which upon equili-
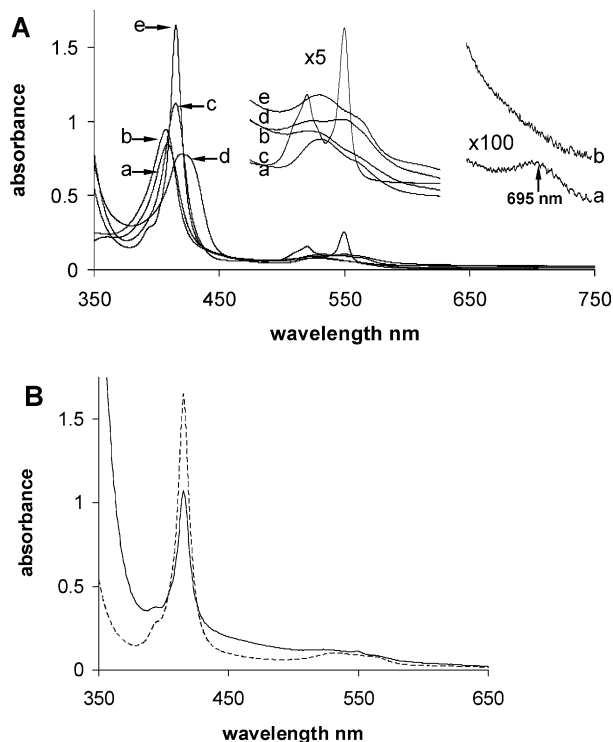
FIGURE 1: (A) Static spectra of cyt c oxidized (a), (a) + addition of a 30-fold molar excess of CL (b), (a) + dithionite (c), (b) + dithionite (d), and (d) + CO (e). Inset: Expanded (×5) visible region of the spectra and expanded (×100) (a) and (b) showing the loss of the 695 nm band for the ferric protein in the presence of CL. Conditions: 8 μM cyt c, 240 μM CL, 1 nM catalase, and 1 mM CO. (B) Cyt c−CO complex formed in the presence of PC/CL liposomes (solid). Conditions: 5 μM cyt c and 180 μM total phospholipid. For comparison, trace e of panel A is also drawn (dashed).
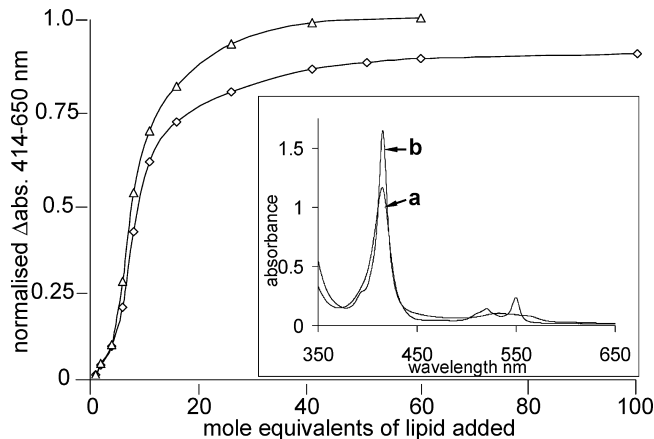

FIGURE 2: Titration of the lipids CL (triangles) and oleate (diamonds) with ferric cyt c, followed by reduction of the protein and addition of CO (differences in the CO spectra were used to ascertain the fraction of lipid bound to protein). Individual spectra were recorded for each lipid concentration and type. 0 mol equiv of lipid corresponds to the fully reduced form and the end of the titration (60 mol equiv of CL and 100 mol equiv of oleate) corresponds to the predominantly CO forms (for CL ~100% as no 550 nm band is present, and for oleate ~90% determined from the amplitude of the 550 nm band remaining). Δabs 414−650 nm normalized such that 0 corresponds to 100% deoxy forms and 1−100% CO forms. Conditions: ~5 μM cyt c and optical path length 1 cm. Inset: Steady-state spectra of (a) reduced cyt c with CO but with no CL (the deoxy form) and (b) reduced cyt c with CO in the presence of 60 mol equiv of CL (the ~100% CO form).

bration with CO forms a derivative having an absorption spectrum typical of CO-bound heme c (20). The transformation of the native protein to this CO-binding form is rapid if CL is added to the conformationally flexible ferric protein which is then reduced and equilibrated with CO. If, alternatively, the ferrous protein is first formed and CL added subsequently, at pH ~7 the transformation takes hours to complete. As it was necessary to add CL dissolved in EtOH to the protein samples, careful controls were carried out adding EtOH alone to cyt c (up to ~5%). In these controls, no spectral changes were observed in either the ferric (e.g., no loss of 695 nm band) or ferrous proteins.

The above experiments were carried out at pH 7.4. We have carried out similar CO binding experiments at considerably lower pH with very similar results (Supporting Information Figure S1, pH 6.1). Thus, CO binding to the cyt c−CL complex can also occur upon acidification of the intermembrane space in respiring mitochondria.

Dynamic light scattering experiments indicated that the CL structures formed in our experiments have an average size of ~90 nm, consistent with lamellar or liposome structures. Figure 1B shows that CO binding to cyt c also occurs in the presence of PC/CL liposomes. In this case, on addition of CO to the cyt c samples the CO adducts were formed in several minutes. For the liposome concentration of Figure 1B (180 μM in total phospholipids) ~90% of the CO adduct of cyt c was formed. The relative scattering background in the cyt c containing PC/CL liposomes was

substantially higher than in cyt c complexed with pure CL (Figure 1B). This feature, as well as the slow (~2 h; see also ref 24) formation of the complexes of cyt c and PC/CL liposomes, makes such structures less suitable for optical studies. Therefore, in the remainder of this work cyt c−CL complexes were used.

The spectral changes that accompany CO addition were used to determine the CL/protein titration curve (Figure 2). This curve is sigmoidal, and full conversion of the protein to the CO binding form is achieved on addition of ~30 CL molecules per cyt c molecule. These would be surprising properties if interpreted as a conventional binding process but are consistent with the formation of lamellar and vesicular structures by the phospholipids (see above) in aqueous dispersion at the concentrations used in our experiments ($>\sim 10^{-6}$ M; see below). Similar lipid/cyt c titrations were observed for cyt c interaction with CL-containing liposomes by Kalanxhi and Wallace (24). Given the critical micelle concentration (cmc) values for other phospholipid molecules of known composition (i.e., chain length and charge of headgroup), a reasonable estimation of the cmc for CL would be in the 10^{-9} M range (25).

Figure 2 also shows that oleate induces the same transition as CL but requires a higher lipid/cyt c ratio for maximum CO binding (~60:1). Oleate was used in this study as a comparison to CL as the acyl chains of both lipids are similar (18 carbon atoms). Interestingly, oleate, like CL, bleaches the 695 nm band indicating loss of the heme−Met80 bond, but even at high oleate/cyt c ratios, where this band was completely diminished, the CO form could not be made to 100%.

Titration of the ferro-cyt c−CL complex with CO (see Supporting Information) yielded equilibrium binding constants (K_b) of 5.5×10^7 M^{-1} (20 °C) and 2.1×10^7 M^{-1} (37 °C) and an estimate for $\Delta H°$ (binding) of ~ -42 kJ mol^{-1}.
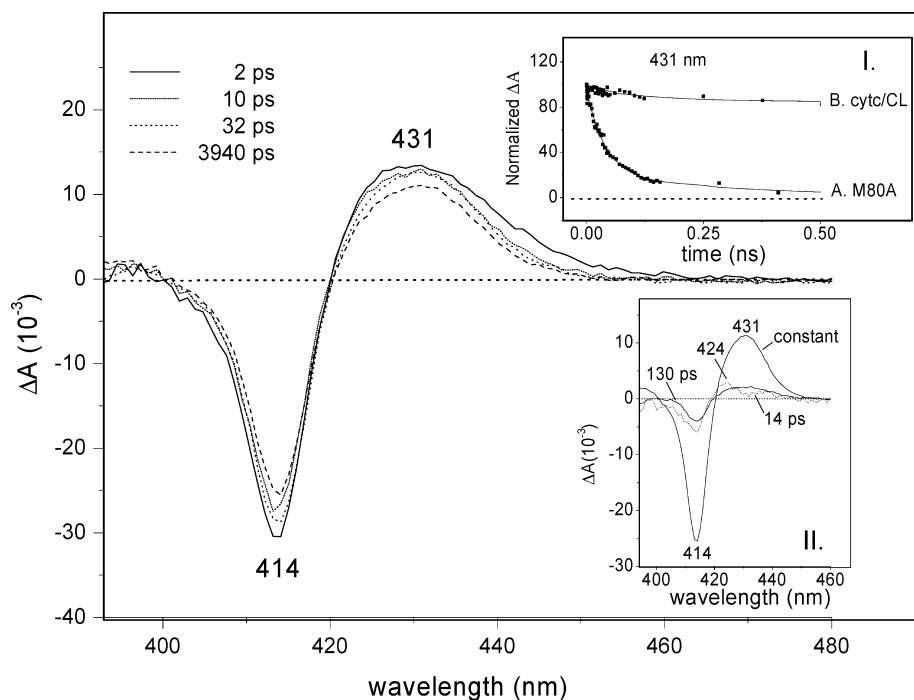
FIGURE 3: Transient absorption spectra of the carbonmonoxy ferro-cyt *c*−CL complex at different delay times in the ps/ns time range. Conditions: 13 μM cyt *c*, 400 μM CL, 1 mM CO, and optical path length 1 mm. Samples were equilibrated for at least 30 min prior to the experiment. Inset I shows the normalized kinetics at 431 nm of the CO-bound complexes of cyt *c*−CL and M80A cyt *c* (taken from ref *16*). Inset II shows the analysis in terms of decay-associated spectra.

These values indicate a high affinity of the complex for CO, very similar to that of Mb ($\sim 3 \times 10^7$ M^{-1} and ~ -44 kJ mol^{-1} (*26*)).

The heme−CO bond can be photolyzed with high quantum yield and the dynamics of CO rebinding followed by transient absorption spectroscopy (*27*). Figure 3 shows the transient absorption spectra in the Soret band region at selected delay times after CO dissociation, in the picosecond and early nanosecond time range. The spectral shape is very similar to that previously reported for CO dissociation from Met80-modified cyt *c* (*15, 16*). Strikingly, however, in contrast to the latter systems, the majority (>80%) of dissociated CO does not rebind on this time scale (Figure 3, inset I).

After a spectral evolution up to a few picoseconds that can be ascribed to heme photophysics (time constant ~ 4 ps), the kinetic trace can be described by two rebinding phases with time constants of 14 ps (7%) and 130 ps (11%) and the main nondecaying phase. The first two phases are ascribed to CO rebinding. The spectrum associated with the 14 ps phase is less red shifted than that of the other phases, indicating that it corresponds to rebinding from a position in which CO still strongly interacts with the heme (*16*). The time constants of the rebinding phases are similar to those reported for chemically (*15*) or genetically (*16*) Met80-modified cyt *c*, but the corresponding amplitudes are much lower and the ~ 1 ns component observed in these systems is completely lacking. Altogether, these experiments demonstrate that CL not only displaces the Met80 heme axial ligand but also allows ligands to escape from the heme environment with a very high yield.

Following photolysis, the fraction of CO that escaped the protein recombined with the heme iron in the microsecond to millisecond time range. Figure 4 illustrates this behavior and also shows that, in agreement with the titration of Figure 1, the amplitude of the recombination increases with the
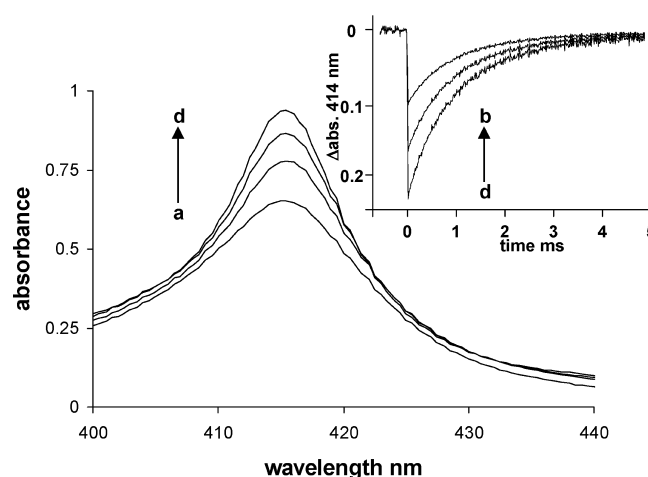

FIGURE 4: The extent of CO binding to ferro-cyt *c* as a function of CL concentration. Steady-state spectra a, b, c, and d correspond to ratios of CL to cyt *c* of 0, 5, 15, and 25, respectively. Inset: Time courses (monitored at 414 nm) b, c, and d correspond to photolysis of CO from the cyt *c*−CL complexes where CL is in 5-, 15-, and 25-fold excess of cyt *c* (see corresponding spectra b−d). The amplitudes of the time courses correspond to $\sim 80\%$ of the total signal (deoxy minus carbonmonoxy) expected from the steady-state spectra. Cyt *c* concentration: 4.8 μM. CO concentration: 100 μM.

concentration of CL, reaching a maximum at ~ 30 CL/cyt *c*. The amplitude of the time course following photodissociation at this maximum CL/cyt *c* ratio corresponds to ~ 0.8 of the absorbance change (deoxy minus carbonmonoxy) expected from the steady-state spectra (Figure 1). This indicates that, in agreement with the ultrafast experiments (Figure 3), most of the CO is photodissociated to bulk solution following a laser flash. The recombination was linearly dependent on CO concentration, yielding a second-order combination constant of 8×10^6 M^{-1} s^{-1}. Stopped-flow experiments mixing the ferro-cyt *c*−CL complex with CO solutions of known

concentrations yielded a very similar value ($\sim 1 \times 10^7$ M^{-1} s^{-1}) for this rate constant.

Independent stopped-flow experiments mixing the carbonmonoxy complex with NO, which replaces CO, gave exponential time courses for this replacement reaction, the rate constants of which were independent of the NO concentration, implying that the determining rate is the first-order dissociation of CO from the heme. This value was determined to be 0.18 s^{-1}. The ratio of the combination to dissociation rate constants yields an equilibrium binding constant $K_b = 4.4 \times 10^7$ M^{-1}, in good agreement with the value obtained at this temperature from the titration data given in Supporting Information Figure S2.

Salt- and detergent-concentration-dependent experiments are described in the Supporting Information. They indicate that the cyt *c*−CL−CO complex is stabilized by interaction between 5−6 positive charges on the surface of cyt *c* and the divalent negative head groups on a CL molecule (see Discussion).

Finally, we investigated the potential role of CO as an inhibitor of peroxidase activity, as previously shown for the cyt *c*−NO complex in the presence of CL (6). Using stopped-flow experiments we observed that upon mixing of the deoxy cyt *c*−CL complex with H$_2$O$_2$ (final concentration 1 mM) heme degradation occurred in majority within 1 s. In the presence of CO (1 or 0.1 mM) this reaction occurred with a rate of 0.0003−0.001 s^{-1}. A similar rate was observed for the reaction of H$_2$O$_2$ with cyt *c* in the absence of CL. We conclude that CO binding to the heme of the cyt *c*−CL complex effectively competes with H$_2$O$_2$ so as to inhibit peroxidase activity.

DISCUSSION

In this work, we describe for the first time the interaction between the cyt *c*−CL complex and the signaling agent CO. Whereas native cyt *c* does not bind CO, we found that CL binding drastically alters this behavior toward exogenous ligand. First it allows CO to bind to the heme, as is the case in genetically or chemically modified cyt *c* proteins where the Met80 residue does not coordinate to the heme, and second it induces in the protein a surprisingly efficient gas exchange channel between the heme environment and solution. In the following we will discuss these properties in detail.

The exact interaction of CL with cyt *c* is not known, since a crystal structure of the complex is lacking. However, electrostatic and hydrophobic interactions are known to take place between CL and cyt *c*. Cyt *c* has a net charge of +8 at physiological pH, allowing electrostatic interactions with the anionic headgroup of CL. The binding surface of cyt *c* includes multiple lysine residues, with residues 72, 73, 86, and 87 as the most frequently identified ones (28−32). Moreover, the Fe−Met80 bond is cleaved (33), alterations are observed in the redox potential, which shifts negatively by 350−400 mV upon binding to CL-containing membranes (4), and tertiary structural changes take place. Based on measurements of temperature-dependent conformational changes at pH 3 in the absence of lipids, it has been suggested that CL binding to cyt *c* induces a conformational switch to a β-sheet structure resulting in heme exposure (34). According to a recent model, a hydrophobic acyl chain of

CL could incorporate into cyt *c* (24). A proposed route for the pivoting acyl chain lies in a crevice that consists of the nonplanar residues comprising the polypeptide strands 67−71 and 82−85 with the positively charged residues Arg91 and Lys72 at either extremity (24).

The CO binding form of the protein that we report here is generated on interaction of an aliphatic hydrocarbon chain of either CL or oleate with the ferric protein and subsequent reduction. The properties of the stability of the complex (Supporting Information) can be understood in the light of the literature discussed above. Addition of detergent to the CO complex abolishes this interaction and allows the ferrous cyt *c* to revert to the native form that is unable to bind CO. CL is more effective than oleate despite the similarity of their acyl chains (both 18 carbon atoms), in part, we presume, because of the electrostatic interactions between the negatively charged phosphate groups on CL and the positive charges on the surface (see Supporting Information). It has also been reported that the type of acyl chain optimal for penetrating cyt *c* is 18:2, as in CL, whereas oleate only has one conjugated bond. Whether this difference is significant for the comparison between CL and oleate in this study is not known (24). Our analysis is consistent with the two negative charges on the CL headgroup interacting with 5−6 positive charges on the surface of the protein. This finding can be understood in terms of the proposal of Kalanxhi and Wallace (24) that there is a specific region of positively charged residues on cyt *c* that binds to CL. The residues identified as being most important in the binding interaction with CL are Lys72, Lys73, Lys86, Lys87, and Arg91, a total of +5 in charge.

The titration curve that we have determined (Figure 2) indicates that cyt *c* interacts not with individual molecules of CL but with lamellar structures formed by CL in aqueous media. A single CL molecule may, therefore, be responsible for the structural changes that are induced in the protein, but the area of the surface that each cyt *c* makes unavailable for further protein molecules to bind comprises $\sim$30 CL molecules. This ratio is generally consistent with a study on the interactions of phospholipid liposomes with cyt *c*, where the maximum effect was attained with a phospholipid/protein ratio of $\sim$30:1 (35).

CO Binding. The second-order rate constant for CO binding to the cyt *c*−CL complex was found to be $\sim 10^7$ M^{-1} s^{-1}. This value is considerably larger than that for myoglobin ($\sim 5 \times 10^5$ M^{-1} s^{-1} (36)) and indeed for any of the different forms of engineered Met80X mutants (1.5×10^4−2.5×10^5 M^{-1} s^{-1} (19)) and cm cyt *c* (1.6×10^6 M^{-1} s^{-1} (20)) produced thus far. This suggests a very open heme crevice in the cyt *c*−CL complex allowing rapid exchange of ligands between the heme "pocket" and the protein environment. An estimate of $\Delta H°$ for CO binding of $\sim$−42 kJ mol^{-1} was obtained. This value lies very close to that measured for CO binding to myoglobin (−44 kJ mol^{-1} (36)) and presumably is determined by formation of the heme−CO bond.

Previous studies of modified forms of cyt *c* (15, 16) have shown the existence and population of several CO docking sites in the protein moiety as indicated by the multiphasic (generally three geminate decay phases) CO rebinding kinetics. The unusually dominant and fast CO rebinding on the picosecond/nanosecond time scale was correlated with

the protein rigidity, which is associated with its electron transfer function (*15, 16*). In the presence of CL, ~20% of the dissociated CO recombines, in a biphasic mode, suggesting the presence of two docking sites. The time constants of 14 and 130 ps are similar to those observed in the chemically modified cyt *c* (16 and 120 ps) and in the Met80Ala mutant (14 and 85 ps), but the amplitudes are much lower (Figure 3). The remaining CO escapes the heme pocket and does not rebind within 4 ns, in contrast to cm cyt *c* and Met80Ala cyt *c*, where substantial CO rebinding occurs on the nanosecond time scale. This comparison indicates that the docking sites corresponding to the fastest decay phases, presumably located in close proximity to the heme, are conserved in the presence of CL. However, the probability of escape from these sites other than via rebinding to the heme is much higher in the presence of CL. Thus CL induces dramatic conformational changes that are not only localized in the distal pocket, as in cm cyt *c* and Met80Ala, but seem to extend to other regions of cyt *c*. The very high escape probability of CO (80%) implies the formation of a ligand exchange pathway, grouping the cyt *c*−CL complex in line with the many ligand-binding heme proteins where CO recombination does not occur or hardly occurs on the picosecond time scale (*27*). This finding is consistent with the loss of properties of cyt *c* as an electron transfer protein and its transformation to a peroxidase (*4, 5*). Studies of NO geminate rebinding to the ferric and ferrous cyt *c*−CL complex also indicate the presence of such a pathway (in preparation).

Implications for the Cyt c-Mediated Apoptotic Pathway. Our study on the steady-state binding of the diatomic ligand CO to the cyt *c*−CL complex and on the ligand binding properties provides valuable insights into the interaction of CL with cyt *c*. The significant conformational changes taking place after binding of CL result in the formation of a channel. This channel should facilitate the access of H_2O_2 to the heme, enabling the peroxidase activity of the cyt *c*−CL complex (*37, 38*). Subsequent oxidation of CL is considered an important step in the apoptotic pathway (*4, 5*). Moreover, the ability of the cyt *c*−CL complex to bind diatomic ligands like CO and NO, which are present in mitochondria (*13, 39*), may be related to a regulatory role of the peroxidase activity of the cyt *c*−CL complex (*6, 10*). There is mounting evidence that CO and NO modulate each other's function within the cell (*10*), suggesting that they may also require each other to initiate apoptosis.

The possible implication of NO−cyt *c* interactions in the early stages of apoptosis has been put forward in previous work by others (*6, 11*). Our present work, showing the unexpectedly high affinity and efficient exchange pathway of CO and its functioning as an inhibitor of peroxidase activity, opens the way to consider a role of CO in the regulation of the initial stages of the apoptotic pathway via its interaction with cyt *c*. An antiapoptotic role of CO has been established (*10, 40, 41*). The mechanisms studied to date concern the later stages of apoptosis, although the primary target of CO, presumably a heme protein, remains to be established. Our study demonstrates that CL raises the affinity of cyt *c* for CO from $\ll 1 \times 10^3$ M^{-1} to ~5×10^7 M^{-1} (half-saturation at 20 nM CO). For comparison the net affinity of the primary target in the respiratory system, cytochrome *c* oxidase, is only ~4×10^6 M^{-1} (*42*). Also, we

are not aware of NO binding curves to cyt *c* in the presence of CL, but half-inhibition of the peroxidase activity of cyt *c* interacting with PC/CL liposomes was reported at NO concentrations of $2.5-4$ μM (*6*).

The physiological CO concentrations in living tissues are not well established but are estimated to lie on average in the low nanomolar range (*43, 44*). This implies that a sizable fraction of CL-anchored cyt *c* may bind CO, thus inhibiting peroxidase activity. The presence of mitochondrial heme oxygenase (*13*) might provide a means to regulate the mitochondrial CO concentration. Altogether, it is reasonable to suggest that CO may also play a role in the regulation of the early stages of apoptosis via its interaction with the cyt *c*−CL complex. As a next step to investigate this possibility, assessments of the interaction of CO with cyt *c* in intact systems are in progress.

SUPPORTING INFORMATION AVAILABLE

CO binding experiments to the cyt *c*−CL complex at pH 6.1, CO titration experiments, and experiments on the stability of the cyt *c*−CL−CO complex in the presence of salt and detergent. This material is available free of charge via the Internet at http://pubs.acs.org.

REFERENCES

1. Flynn, P. F., Bieber Urbauer, R. J., Zhang, H., Lee, A. L., and Wand, A. J. (2001) Main chain and side chain dynamics of a heme protein: ^{15}N and ^{2}H NMR relaxation studies of *R. capsulatus* ferrocytochrome *c*₂. *Biochemistry 40*, 6559–6569.
2. Louie, G. V., and Brayer, G. D. (1990) High-resolution refinement of yeast iso-1-cytochrome *c* and comparisons with other eukaryotic cytochromes *c*. *J. Mol. Biol. 214*, 527–555.
3. Ow, Y.-L. P., Green, D. R., Hao, Z., and Mak, T. W. (2008) Cytochrome *c*: Functions beyond respiration. *Nat. Rev. Mol. Cell. Biol. 9*, 532–542.
4. Basova, L. V., Kurnikov, I. V., Wang, L., Ritov, V. B., Belikova, N. A., Vlasova, I. I., Pacheco, A. A., Winnica, D. E., Peterson, J., Bayir, H., Waldeck, D. H., and Kagan, V. E. (2007) Cardiolipin switch in mitochondria: Shutting off the reduction of cytochrome *c* and turning on the peroxidase activity. *Biochemistry 46*, 3423–3434.
5. Belikova, N. A., Vladimirov, Y. A., Osipov, A. N., Kapralov, A. A., Tyurin, V. A., Potapovich, M. V., Basova, L. V., Peterson, J., Kurnikov, I. V., and Kagan, V. E. (2006) Peroxidase activity and structural transitions of cytochrome *c* bound to cardiolipin-containing membranes. *Biochemistry 45*, 4998–5009.
6. Vlasova, I. I., Tyurin, V. A., Kapralov, A. A., Kurnikov, I. V., Osipov, A. N., Potapovich, M. V., Stoyanovsky, D. A., and Kagan, V. E. (2006) Nitric oxide inhibits peroxidase activity of cytochrome *c*·cardiolipin complex and blocks cardiolipin oxidation. *J. Biol. Chem. 281*, 14554–14562.
7. Krebs, J. J. R., Hauser, H., and Carafoli, E. (1979) Asymmetric distribution of phospholipids in the inner membrane of beef-heart mitochondria. *J. Biol. Chem. 254*, 5308–5316.
8. Daum, G. (1985) Lipids of mitochondria. *Biochim. Biophys. Acta 822*, 1–42.
9. Chung, H. T., Pae, H. O., Choi, B. M., Billiar, T. R., and Kim, Y. M. (2001) Nitric oxide as a bioregulator of apoptosis. *Biochem. Biophys. Res. Commun. 282*, 1075–1079.
10. Bilban, M., Haschemi, A., Wegiel, B., Chin, B. Y., Wagner, O., and Otterbein, L. E. (2008) Heme oxygenase and carbon monoxide initiate homeostatic signaling. *J. Mol. Med. 86*, 267–279.
11. Schonhoff, C. M., Gaston, B., and Mannick, J. B. (2003) Nitrosylation of cytochrome *c* during apoptosis. *J. Biol. Chem. 278*, 18265–18270.
12. Boczkowski, J., Poderoso, J. J., and Motterlini, R. (2006) CO-metal interaction: vital signaling from a lethal gas. *Trends Biochem. Sci. 31*, 614–621.
13. Converso, D. P., Taille, C., Carreras, M. C., Jaitovich, A., Poderoso, J. J., and Boczkowski, J. (2006) HO-1 is located in liver

mitochondria and modulates mitochondrial heme content and metabolism. *FASEB J. 20*, 1236–1238.

14. Moore, T. A., Greenwood, C., and Wilson, M. T. (1975) Ligand binding to ferrocytochrome *c* at high pH. *Biochem. J. 147*, 335–341.

15. Silkstone, G., Jasaitis, A., Vos, M. H., and Wilson, M. T. (2005) Geminate carbon monoxide rebinding to a *c*-type haem. *Dalton Trans. 21*, 3489–3494.

16. Silkstone, G., Jasaitis, A., Wilson, M. T., and Vos, M. H. (2007) Ligand dynamics in an electron-transfer protein: picosecond geminate recombination of carbon monoxide to heme in mutant forms of cytochrome *c*. *J. Biol. Chem. 282*, 1638–1649.

17. Goto, Y., Hagihara, Y., Hamada, D., Hoshino, M., and Nishii, I. (1993) Acid-induced unfolding and refolding transitions of cytochrome *c*: A three-state mechanism in water and deuterium oxide. *Biochemistry 32*, 11878–11885.

18. Dalziel, K., and O'Brien, J. R. (1957) Side reactions in the deoxygenation of dilute oxyhaemoglobin solutions by sodium dithionite. *Biochem. J. 67*, 119–124.

19. Silkstone, G., Stanway, G., Brzezinski, P., and Wilson, M. T. (2002) Production and characterisation of Met80X mutants of yeast iso-1-cytochrome *c*: Spectral, photochemical and binding studies on the ferrous derivatives. *Biophys. Chem. 98*, 65–77.

20. Wilson, M. T., Brunori, M., Rotilio, G. C., and Antonini, E. (1973) Properties of modified cytochromes. II. Ligand binding to reduced carboxymethyl cytochrome *c*. *J. Biol. Chem. 248*, 8162–8169.

21. Othman, S., Le Lirzin, A., and Desbois, A. (1993) A heme *c*-peptide model system for the resonance Raman study of *c*-type cytochromes: Characterization of the solvent-dependence of peptide-histidine-heme interactions. *Biochemistry 32*, 9781–9791.

22. Droghetti, E., Oellerich, S., Hildebrandt, P., and Smulevich, G. (2006) Heme coordination states of unfolded ferrous cytochrome *c*. *Biophys. J. 91*, 3022–3031.

23. Andrew, C. R., George, S. J., Lawson, D. M., and Eady, R. R. (2002) Six- to five-coordinate heme-nitrosyl conversion in cytochrome *c*′ and its relevance to guanylate cyclase. *Biochemistry 41*, 2353–2360.

24. Kalanxhi, E., and Wallace, C. J. A. (2007) Cytochrome *c* impaled: Investigation of the extended lipid anchorage of a soluble protein to mitochondrial membrane models. *Biochem. J. 407*, 179–187.

25. Cevc, G., Ed. (1993) *Phospholipid Handbook*, Marcel Dekker, New York.

26. Springer, B. A., Egeberg, K. D., Sligar, S. G., Rohlfs, R. J., Mathews, A. J., and Olson, J. S. (1989) Discrimination between oxygen and carbon monoxide and inhibition of autooxidation by myoglobin. Site-directed mutagenesis of the distal histidine. *J. Biol. Chem. 264*, 3057–3060.

27. Vos, M. H. (2008) Ultrafast dynamics of ligands within heme proteins. *Biochim. Biophys. Acta 1777*, 15–31.

28. Huang, Y. Y., and Kimura, T. (1984) Thermodynamic parameters for the reduction reaction of membrane-bound cytochrome-*c* in comparison with those of the membrane-free form: Spectropotentiostatic determination with use of an optically transparent thin-layer electrode. *Biochemistry 23*, 2231–2236.

29. Gorbenko, G. P., and Domanov, Y. A. (2003) Cytochrome *c* location in phosphatidylcholine/cardiolipin model membranes: Resonance energy transfer study. *Biophys. Chem. 103*, 239–249.

30. Gorbenko, G. P., Molotkovsky, J. G., and Kinnunen, P. K. J. (2006) Cytochrome *c* interaction with cardiolipin/phosphatidylcholine model membranes: Effect of cardiolipin protonation. *Biophys. J. 90*, 4093–4103.

31. Kawai, C., Prado, F. M., Nunes, G. L. C., Di Mascio, P., Carmona-Ribeiro, A. M., and Nantes, I. L. (2005) pH-dependent interaction of cytochrome *c* with mitochondrial mimetic membranes−The role of an array of positively charged amino acids. *J. Biol. Chem. 280*, 34709–34717.

32. Kostrzewa, A., Pali, T., Froncisz, W., and Marsh, D. (2000) Membrane location of spin-labeled cytochrome *c* determined by paramagnetic relaxation agents. *Biochemistry 39*, 6066–6074.

33. Kagan, V. E., Tyurin, V. A., Jiang, J. F., Tyurina, Y. Y., Ritov, V. B., Amoscato, A. A., Osipov, A. N., Belikova, N. A., Kapralov, A. A., Kini, V., Vlasova, I. I., Zhao, Q., Zou, M. M., Di, P., Svistunenko, D. A., Kurnikov, I. V., and Borisenko, G. G. (2005) Cytochrome *c* acts as a cardiolipin oxygenase required for release of proapoptotic factors. *Nat. Chem. Biol. 1*, 223–232.

34. Balakrishnan, G., Hu, Y., Oyerinde, O. F., Su, J., Groves, J. T., and Spiro, T. G. (2007) A conformational switch to beta-sheet structure in cytochrome *c* leads to heme exposure. Implications for cardiolipin peroxidation and apoptosis. *J. Am. Chem. Soc. 129*, 504–505.

35. Tuominen, E. K. J., Wallace, C. J. A., and Kinnunen, P. K. J. (2002) Phospholipid-cytochrome *c* interaction. Evidence for the extended lipid anchorage. *J. Biol. Chem. 277*, 8822–8826.

36. Antonini, E., and Brunori, M. (1971) *Hemoglobin and myoglobin in their reactions with ligands*, North-Holland, Amsterdam.

37. Kapralov, A. A., Kurnikov, I. V., Vlasova, I. I., Belikova, N. A., Tyurin, V. A., Basova, L. V., Zhao, Q., Tyurina, Y. Y., Jiang, J. F., Bayir, H., Vladimirov, Y. A., and Kagan, V. E. (2007) The hierarchy of structural transitions induced in cytochrome *c* by anionic phospholipids determines its peroxidase activation and selective peroxidation during apoptosis in cells. *Biochemistry 46*, 14232–14244.

38. Vladimirov, Y. A., Proskurnina, E. V., Izmailov, D. Y., Novikov, A. A., Brusnichkin, A. V., Osipov, A. N., and Kagan, V. E. (2006) Cardiolipin activates cytochrome *c* peroxidase activity since it facilitates H_2O_2 access to heme. *Biochemistry (Moscow) 71*, 998–1005.

39. Ghafourifar, P., and Cadenas, E. (2005) Mitochondrial nitric oxide synthase. *Trends Pharmacol. Sci. 26*, 190–195.

40. Brouard, S., Berberat, P. O., Tobiasch, E., Seldon, M. P., Bach, F. H., and Soares, M. P. (2002) Heme oxygenase-1-derived carbon monoxide requires the activation of transcription factor NF-kappa B to protect endothelial cells from tumor necrosis factor-alpha-mediated apoptosis. *J. Biol. Chem. 277*, 17950–17961.

41. Zhang, X. C., Shan, P. Y., Alam, J., Fu, X. Y., and Lee, P. J. (2005) Carbon monoxide differentially modulates STAT1 and STAT3 and inhibits apoptosis via a phosphatidylinositol 3-kinase/Akt and p38 kinase-dependent STAT3 pathway during anoxia-reoxygenation injury. *J. Biol. Chem. 280*, 8714–8721.

42. Einarsdottir, O. (1995) Fast reactions of cytochrome oxidase. *Biochim. Biophys. Acta 1229*, 129–147.

43. Piantadosi, C. A. (2002) Biological chemistry of carbon monoxide. *Antioxid. Redox Signal. 4*, 259–270.

44. Wu, L., and Wang, R. (2005) Carbon monoxide: Endogenous production, physiological functions, and pharmacological applications. *Pharmacol. Rev. 57*, 585–630.